NONIDEALITY OF VOLUME FLOWS AND PHASE TRANSITIONS OF F-ACTIN SOLUTIONS IN RESPONSE TO OSMOTIC STRESS

TADANAO ITO, KEN S. ZANER, and THOMAS P. STOSSEL
Hematology-Oncology Unit, Massachusetts General Hospital, Department of Medicine, Harvard Medical School, Boston, Massachusetts 02114

ABSTRACT Ovalbumin and G-actin solutions decreased their volume in a concentration-dependent manner in response to an osmotic stress, arising from an osmotic pressure gradient of 5–20 cm H_2O at 25°C, at protein concentrations as high as 20 mg/ml. In contrast, solutions of F-actin exhibited a concentration-dependent decrease in their rate of volume change in response to the osmotic stress. Shortening of F-actin by gelsolin did not affect this decrease, suggesting that the elastic response of the filaments underlies the osmotically nonideal behavior. However, above a critical actin concentration of ~7 mg/ml, no volume change occurred in response to osmotic gradients as high as 20 cm H_2O. The concentration at which this critical phenomenon occurred and its abolition by shortening of F-actin by gelsolin suggest that a transition of diffusible rods to a glassy state is the cause of this critical phenomenon. Above the critical concentration, an increase in the osmotic pressure applied to an F-actin solution to >20 cm H_2O produced a transient increase in flow rate to that expected for a solution containing no polymer. This finding may represent a transition from an isotropic glassy state to an anisotropic and heterogeneous one wherein regions of pure solvent coexist with domains of pure polymer.

INTRODUCTION

The periphery of many eukaryotic cells contains a network composed of actin filaments (F-actin). Actin networks can be likened to other polymer systems that have certain mechanical properties in response to imposed forces that depend on the length, concentration, and degree of cross-linking of the polymer molecules. These mechanical properties probably are important in the maintenance of cell shape and the mechanism of cell movement (reviewed by Stossel, 1984). Polymer networks can also swell or contract in response to an osmotic gradient (Tanaka and Fillmore, 1979; Tanaka, 1981). Since cells undergo swelling and compression in response to environmental osmotic stresses, the osmotic properties of actin networks are also likely to be important for cell structure and function.

This paper presents the first efforts toward an experimental and theoretical analysis of the osmotic behavior of actin. A method that measures water flow in an osmotically stressed polymer solution is described, and evidence that purified filamentous, but not monomeric, actin exerts a concentration-dependent elastic response to osmotic stress is presented. The elastic resistance also demonstrates critical concentration and osmotic stress-dependent behavior indicative of phase transitions. The theoretical analysis presented in the accompanying Appendix provides a thermodynamic interpretation of actin filament solutions subjected to osmotic stress requiring no special assumptions about their mechanical properties.

Dr. Ito's present address is Department of Biophysics, Faculty of Sciences, Kyoto University, Kyoto, Japan.

Correspondence should be addressed to Dr. Zaner.

MATERIALS AND METHODS

Materials

Monomeric actin (G-actin) was prepared from rabbit skeletal muscle by the method of Spudich and Watt (1971). Dextran (average molecular weight, 40,000) from Sigma Chemical Co. (St. Louis, MO) was used without further purification. Gelsolin was prepared from human plasma as described by Chapponier et al. (1986).

Osmometer

The osmometer is similar in design to that of Zimm and Myerson (1946) but is smaller and was fabricated from Lucite. A diagram of the device is shown in Fig. 1. Acetyl cellulose membranes (Schleicher & Schuell, Inc., Keene, NH), which have a nominal protein retention of 20 kD, are clamped between rubber gaskets held in place by the screw on a Lucite cap. The volume of the membrane-enclosed chamber (compartment I) is 1.5 ml. The capillary tube (50 μl micropipet, Corning Glass Works, Corning Science Products, Corning, NY) and the fill port are held in place by gaskets.

Samples are introduced into the chamber through the fill port, which is then clamped shut. After inspecting the osmometer for the presence of leaks or air bubbles, it is placed in the outer chamber (compartment II), which contains 500 ml of buffer. The temperature of this chamber is controlled within 0.1°C by a water jacket that is connected to a thermostatically controlled circulator.

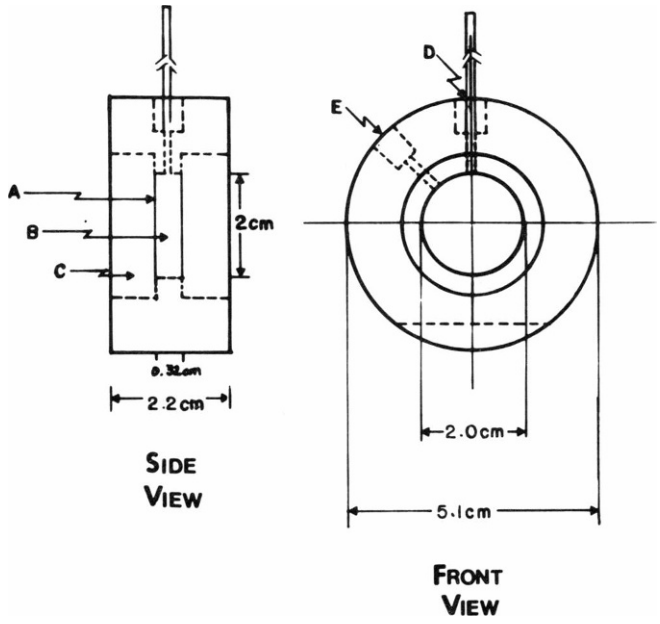

FIGURE 1 Schematic of the Osmometer. (*A*) Dialysis membranes. Each membrane is supported by a perforated plastic grating to prevent swelling of the membrane by hydrostatic pressure and is gasketted in place. (*B*) Compartment I, which is the chamber bounded by the dialysis membranes and is continuous with the capillary. (*C*) Compartment II, which is external to the membranes and is continuous with the large external bath. (*D*) Capillary tube, which is a 50 μl micropipet. (*E*) Fill port.

Volume Flow Measurements

A typical volume flow measurement proceeds as follows: 1.5 ml of G-actin in the low ionic strength buffer solution A of Spudich and Watt (2 mM Tris-HCl, 0.5 mM ATP, 0.2 mM $CaCl_2$, 0.5 mM β-mercaptoethanol, pH 8.0) containing 20 mg/ml of dextran is injected into the osmometer. The osmometer assembly is then placed in the jacketed outer chamber, which contains a different buffer solution (10 mM imidazole-HCl, 0.2 mM $CaCl_2$, 0.2 mM ATP, 0.1 M KCl, 2 mM $MgCl_2$, pH 7.5). The sample is then incubated overnight at 4°C during which time the $MgCl_2$ entering compartment I causes the actin to polymerize. In addition, there is an increase in volume in compartment I due to the difference in osmotic strength, which leads to an increase in the hydrostatic pressure difference. The temperature is then increased to 25°C and the system is incubated for several hours at this temperature to achieve equilibrium at which time the hydrostatic pressure difference is ~20 cm H_2O. The osmolarity of the buffer in the outer chamber is then changed by removing a precise volume of solution and adding the same volume of 200 mg/ml dextran dissolved in the same buffer solution. The change in the position of the meniscus in the capillary following the osmolarity change is measured by a ruler attached to the capillary and the time course is recorded. Volume flow is determined from the slope of the time course at steady state. After enough points have been obtained for an accurate determination of the flow rate, the osmolarity is changed again in the manner described above. The procedure is them repeated four to five times on the same sample to obtain the relationship between flow and osmotic stress.

RESULTS

If a solution behaves ideally in response to an osmotic stress, the volume flow, J_v, is

$$J_v = L_p P_f,$$

where P_f is the osmotic stress and L_p is the filtration coefficient of the membrane (Katchalsky and Curran, 1965). The osmotic stress, P_f, is determined from

$$P_f = \Delta P_h - RT\Delta C,$$

where ΔP_h is the hydrostatic pressure difference, ΔC is the difference in molar concentration between the two compartments, and R and T have their usual meaning. P_f is, therefore, the thermodynamic drive that causes water to flow from compartment I to compartment II, and that becomes zero at equilibrium.

The time course of water flow for 20 mg/ml of dextran under various osmotic stresses is shown in Fig. 2. The flow rate becomes constant within 10 min after changing the osmolarity of the outside solution at time zero. Volume flow was calculated from the slope of the line at a constant flow rate. As shown in Fig. 3, the volume flow, J_v, was directly proportional to the osmotic stress, P_f, below 30 cm H_2O and was identical for different membranes of the same lot. The slope was independent of the dextran concentration in the test solution below 30 mg/ml, which implies that the dextran solution behaves as an osmotically ideal solution. The filtration coefficient, L_p, calculated from the slope is 4.7×10^{-10} cm^5/dyn s. In most of the experiments to be described, 20 mg/ml of dextran was added to the actin. This concetration of dextran had no effect on the extent of polymerization of actin as assessed by its gelation

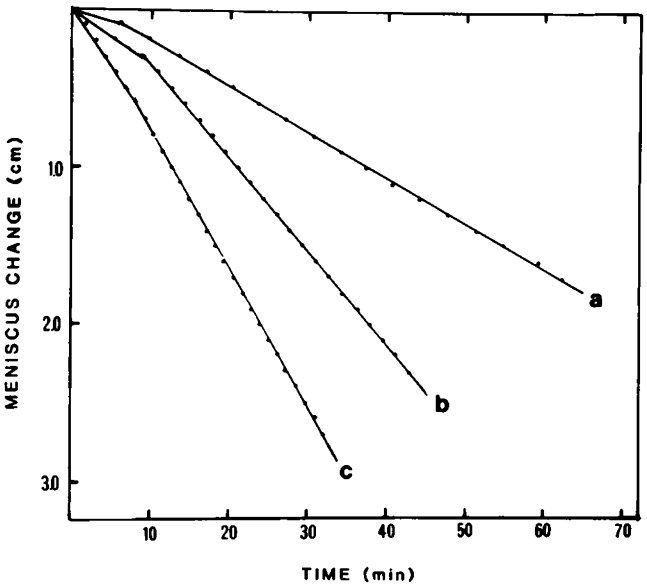

FIGURE 2 Time course of the volume change of a 20 mg/ml dextran solution. The change in height of the meniscus in the capillary as a function of time is plotted for various intensities of osmotic stress, P_f. The change in volume is proportional to the meniscus change in the capillary. The intensities of P_f are 7.8 cm H_2O (*a*), 15.4 cm H_2O (*b*), and 22.5 cm H_2O (*c*), respectively. The buffer composition in compartment II is 10 mM imidazole HCl, 0.2 mM $CaCl_2$, 0.2 mM ATP, 0.1 M KCl, 2 mM $MgCl_2$, pH 7.5 at 25°C.

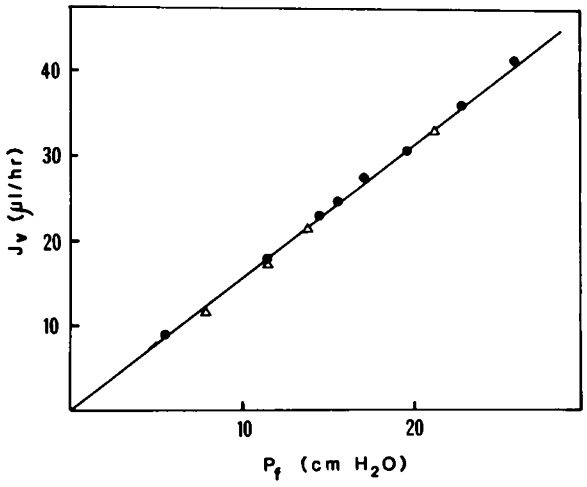

FIGURE 3 The dependence of volume flow on osmotic stress of a 20 mg/ml dextran solution. The volume flow, J_v, of a 20 mg/ml dextran solution is calculated from the slope of the volume change at steady state as shown in Fig. 2. The values are plotted against various intensities of the osmotic stress, P_f. The different symbols represent different membranes of the same lot.

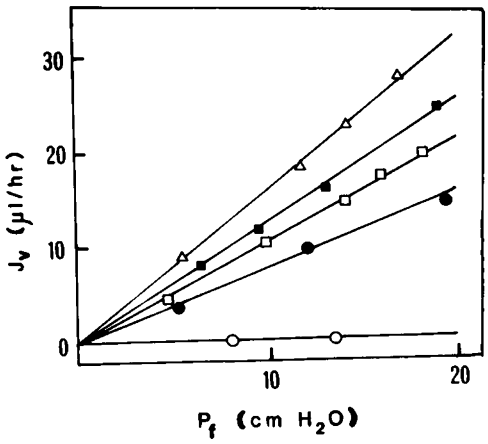

FIGURE 5 Dependence of volume flow on the osmotic stress of F-actin solutions. The volume flow of various concentrations of F-actin are plotted against the osmotic stress, P_f. The concentrations are 0 mg/ml (△), 3.3 mg/ml (■), 5.5 mg/ml (□), 6.5 mg/ml (●), and 7.7 mg/ml (○). The buffer composition in compartment II is the same as in Fig. 2.

by macrophage actin-binding protein measured by viscometry (data not shown).

The relationship between volume flow and the osmotic stress for solutions containing 6.1 or 4.0 mg/ml of G-actin is shown in Fig. 4. The slope is not different from that of a dextran solution and is independent of the concentrations of G-actin tested. These results show that G-actin solutions behave as an osmotically ideal solution in response to osmotic stress. 10 mg/ml ovalbumin and 9 mg/ml bovine serum albumin also had no effect on volume flow.

However, the flow properties observed when F-actin is in the osmometer are quite different. In this case (Fig. 5), the volume flow rate increases in direct proportion to the osmotic stress below 20 cm H_2O, with a slope less than that observed for G-actin. Moreover, the slope decreases as the concentration of F-actin rises. Above F-actin concentrations of ~7 mg/ml there is no flow. Since L_p is a constant that is characteristic of the membrane, these results can be represented as

$$J_v = L_p (1 - \epsilon) P_f, \quad (1)$$

where ϵ is an empirical parameter that quantitates the nonideality of volume flow of an actin solution in response to the osmotic stress, P_f. ϵ varies monotonically with the

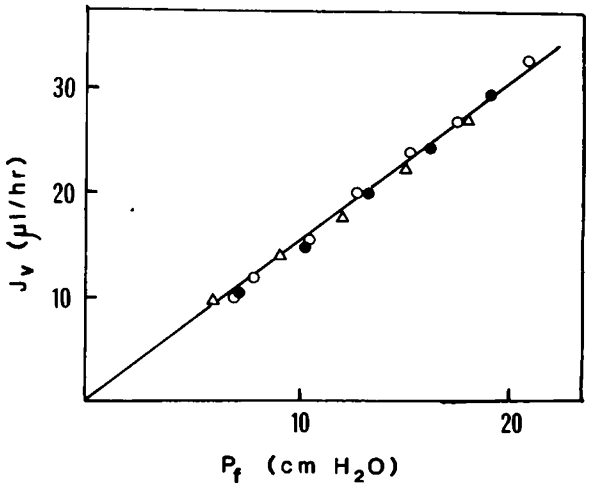

FIGURE 4 Dependence of volume flow on the osmotic stress of G-actin solutions. The volume flow, J_v, of different concentrations of G-actin are plotted against the osmotic stress, P_f. The concentrations are: 0 mg/ml (●), 4.0 mg/ml (○), and 6.1 mg/ml (△), respectively. The buffer composition in compartment II is 2 mM Tris-HCl, 0.5 mM ATP, 0.2 mM $CaCl_2$, pH 7.7 at 25°C.

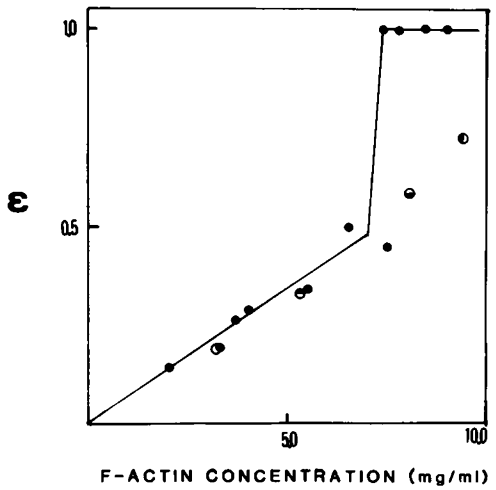

FIGURE 6 The dependence of ϵ on the F-actin concentration in the presence and absence of gelsolin. The values of ϵ, obtained from the slope of a P_f vs. J_v curve, such as shown in Fig. 5, are plotted against the concentrations of F-actin. F-actin without added gelsolin (●); F-actin in the presence of gelsolin at molar ratios to actin of 66:1 (○), 330:1 (⊖), 800:1 (⊖), and 350:1 (◐).

F-actin concentration but is independent of the osmotic stress. The value of ϵ can be obtained from Eq. 1 by measuring the slope of the curve of J_v vs. P_f at a given concentration of F-actin.

The value of ϵ as a function of the F-actin concentration is shown in Fig. 6. ϵ increases in direct proportion to the F-actin concentration <7 mg/ml. The abrupt increase of ϵ to unity, which occurs above this concentration, suggests some type of phase transition. When the length of the actin filaments are shortened by the F-actin-severing protein, gelsolin, ϵ increases continuously as a function of actin concentration and does not exhibit the abrupt change observed in the absence of gelsolin. Furthermore, gelsolin does not change the F-actin concentration dependence of the slope of ϵ.

The narrow concentration range over which the value of ϵ can abruptly rise is illustrated by the data in Fig. 7. In this experiment, volume flow was observed at progressively increasing osmotic stresses. The flow rate increased at the lower osmotic stress intensities but then decreased at higher intensities. This result presumably reflects a small but finite increase in the actin concentration, which is poised at the critical point. This change in the actin concentration was estimated and the relationship between ϵ and the actin concentration, shown in Fig 7 (*inset*), indicates that a change of 0.1 mg/ml in concentration is sufficient to induce the abrupt change in ϵ. The concentration at which the transition occurred was somewhat lower than 7.0 mg/ml measured in the experiment in Fig. 6. This slight discrepancy probably reflects variations in average filament lengths in different experiments in the setting of a strong dependence of this type of transition on the filament length.

This cessation of flow above a critical concentration only occurs below a critical intensity of osmotic stress. When the osmotic stress was raised above this level there was a transient large increase in the flow which, at steady state, reaches a rate close to that of an F-actin-free solution. The time course of the change in meniscus height, which is equivalent to the flow, following the application of a greater force is shown in Fig. 8. The critical osmotic stresses were <20 cm H_2O, and the lowest was 13.8 cm H_2O for a 7.4 mg/ml concentration of F-actin. The ratio of the flow rate for a solution containing F-actin at a higher osmotic stress to that of an F-actin-free solution was 0.87 at 20 cm H_2O and 1.0 at 35 cm H_2O. The effect of pressure was reversible. When, after application of osmotic stress above the critical concentration, the force was decreased, there was a large decrease in volume flow and the ratio became 0.25 at 10 cm H_2O.

A similar abrupt change in volume flow was also observed for F-actin solutions in which there was flow at all osmotic stress intensities. With low F-actin concentrations, the change was less obvious than those above the critical concentration, but the same large flow was clearly observed as in the solutions containing the high F-actin concentrations in which the flow was produced by gelsolin (Fig. 8).

DISCUSSION

Polymer gels alter their volume in response to an osmotic pressure difference between the inside and outside of the gel. The osmotic stress deforms the filaments that make up the gel thus creating an elastic pressure that counteracts the applied osmotic pressure. It is reasonable to expect that gels composed of the biopolymer F-actin would exhibit

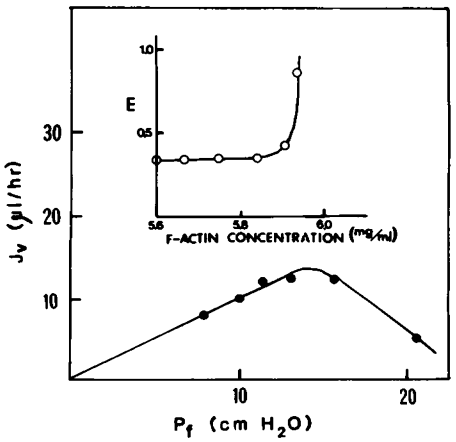

FIGURE 7 Volume flow of an F-actin solution close to the critical concentration. The volume flow, J_v, of 5.6 mg/ml F-actin solution is plotted against the osmotic stress, P_f. (*Inset*) The concentrations of F-actin are estimated by calculating the concentration change following the volume change. The buffer composition in compartment II is the same as in Fig. 2.

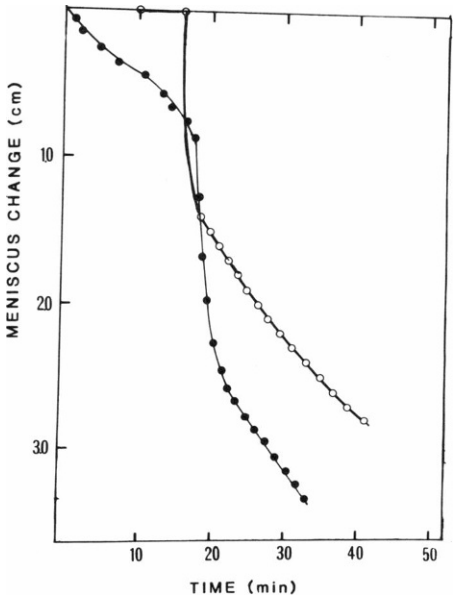

FIGURE 8 Rapid volume flow of F-actin solution induced by rapid increment in osmotic stress. The volume flow is plotted as a function of time either for a 7.7 mg/ml F-actin solution (○) or for a 9.4 mg/ml F-actin solution containing 0.54 mg/ml gelsolin (●). The buffer composition in compartment II is the same as in Fig. 2.

such behavior, and that such gels might be of importance in the volume regulation of the living cell. The data presented in this report demonstrate that F-actin responds nonideally to an osmotic stress in a concentration and length-dependent fashion, which is probably due to the elastic properties of the filaments.

The experimental results indicate that purified actin can exist in several states as defined by its osmotic responses. As expected from most previous work, solutions of G-actin and of serum and egg albumin behaved as osmotically ideal solutions. In contrast, when G-actin was polymerized into F-actin, it did not respond ideally to an osmotic stress. At concentrations <7 mg/ml, the rate of water flow decreased in a concentration-dependent, but filament-length independent, manner. Above 7 mg/ml there was no flow observed below a pressure of ~20 cm H_2O, but, at higher pressures, a transient large flow occurred, followed by a steady-state flow about equal to that observed for the nonfilamentous systems.

The decrease of volume flow caused by the presence of actin filaments might be due to the frictional forces between the solvent and the filaments. That the volume flow decreases upon polymerization suggests that the frictional forces between the solvent and the actin monomers, which should be independent of the state of polymerization, are not responsible for the decrease in flow rate. In addition, the analysis in the Appendix shows that the frictional force between the solvent and the filaments is negligible in the F-actin solutions under the experimental conditions.

Alternatively, the decrease in volume flow may be due to an elastic response of the filaments to the applied osmotic stress as further discussed in the Appendix. The osmotic stress does osmotic work, which both removes water across the membrane and also compresses the filaments. Some of the energy is dissipated by the frictional interaction between the water molecules and the membrane while the remainder is stored in the free energy of deformation of the filaments, which produces an elastic pressure in the solution. This elastic pressure decreases the chemical potential difference between the inside and the outside of the chamber, thus decreasing the driving force for volume flow (Katchalsky and Curran, 1965). As discussed in the Appendix, the elastic pressure, ΔP_e, is linearly proportional to the applied stress, P_f, with the proportionality constant, ϵ, which corresponds to the empirical parameter that quantitates the nonideality of volume flow. That ϵ increases linearly with increasing actin concentration and is independent of the shortening of the filaments by gelsolin below 7 mg/ml suggests that the osmotic compressibility of the filaments is independent of the concentration and length.

At concentrations where there is complete elimination of flow, the diffusion of the filaments is inhibited, but they can still be compressed by the osmotic stress. There is, therefore, no dissipation of energy by volume flow as discussed above and there is an abrupt increase in the elastic pressure, which is reflected by a sudden increase of ϵ to unity at this point. Such a phenomenon is consistent with the prediction by Edwards and Evans (1982) that rods in concentrated solution undergo a kind of glassy transition when the quantity $cdl^2 = \gamma$ approaches unity, where c is the concentration, l is the length, and d is the filament thickness. This glassy state is characterized by the fact that diffusional freedom along the long axis is inhibited, although short range compression or bending is permitted. γ is greater than unity at a filament length >1 μm, a diameter of 5.0 nm, and a concentration of 6 mg/ml. That the shortening of the filament length by gelsolin eliminates the discontinuity in flow is also consistent with the idea of a glassy transition.

This complete elimination of flow occurs at osmotic stresses below 20 cm H_2O. At higher stresses there is a transient large flow followed by a steady state flow close to that of the nonfilamentous solutions. This phenomenon may be the result of a phase transition from an isotropic to an anisotropic state. Under physiologic conditions (of osmotic stress, salt concentration, pH, etc.), actin filaments are distributed relatively isotropically, have minimum contact with one another, and are, therefore, surrounded extensively by solvent. The increase in osmotic stress creates a progressively more unstable situation that can culminate in a transition to another state in which the filaments are less surrounded by solvent, for example, a crystalline-like state. That the steady-state flow after this transition is nearly equal to the flow of an F-actin-free solution suggests the existence of a heterogeneous state in which a nearly pure solvent phase is separated from a more concentrated filament phase. In this state the chemical potential of water is almost equivalent to that of the pure solvent. The large transient flow accompanying the transition arises from the discontinuity in the chemical potential of water at the membrane boundary made by the transition. This transient discontinuity can also be observed in systems where there is flow at all values of the osmotic stress, as is the case for F-actin in the presence of gelsolin.

This transition may correspond to the phase transition predicted theoretically by Flory (1956*a*, *b*) in his analysis of the thermodynamic properties of rigid, solvent-impenetrable rods. His analysis showed that a small increase in the rod–rod interaction energy, χ, which is defined as the energy change upon transferring a rod from a solution to infinite dilution, can cause a homogeneous system to form a two-phase system consisting of a nearly pure filament phase and a nearly pure solvent phase. It is possible that in the present system χ is replaced by P_f^2, which, as further discussed in the Appendix, is proportional to the energy of deformation.

Since the shortening of actin filaments by gelsolin increases the actin concentration at which volume flow is eliminated, it would be suspected that lengthening of the filaments, by subjecting the actin to further purification by

gel filtration (Zaner and Stossel, 1982), would decrease the actin concentration at which this phenomenon occurs. Our preliminary data suggest that this is true (Ito, T., K. S. Zaner, and T. P. Stossel, manuscript in preparation) and, moreover, this is consistent with the data of Tait and Frieden (1982) who demonstrated, by fluorescence photobleaching recovery, that gel-filtered actin at a concentration of 1 mg/ml was immobilized. The observed immobilization of the filaments is somewhat in contrast to previous rheologic measurements, which have been interpreted in terms of a model of noninteracting interpenetrating rods (Zaner and Stossel, 1983). The discrepancy is probably due to the fact that the mechanical properties of F-actin in simple shear are dictated by the rotational freedom of the filaments, whereas in the present study, it is the translational diffusion that is of most importance. The data suggest that there is a much larger resistance to an isotropic volume change than there is to pivotting of the filaments by a shear force.

If the actin network in the periphery of cells exhibits elastic resistance to osmotic perturbation, this could play an important role in cell volume regulation. The results described in this paper indicate that filamentous, but not monomeric, actin responds nonideally to osmotic stress. Actin filaments crosslinked by gelation proteins would be expected to show even greater osmotic resistance, and our preliminary studies indicate that macrophage actin-binding protein markedly increases the osmotic resistance of F-actin (Ito, T., K. S. Zaner, and T. P. Stossel, manuscript in preparation).

The results with F-actin presented here as well as rheological studies (Zaner and Stossel, 1983; Zaner, 1986) indicate that actin networks are best characterized as interpenetrating rods. In contrast to flexible chains, rods will show an enthalpic rather than entropic response to either mechanical or osmotic stress without any significant volume change. Therefore, the swelling properties of a gel made of rods may be quite different from those made of flexible chains. The findings reported here also suggest that theoretical models of cell movement based on the swelling behavior of cytoplasmic matrices need to be reevaluated because these models assume that cytoplasmic networks have the elastic properties of flexible rubber networks (Schmid-Schonbein et al., 1981; Oster, 1984; Oster and Perelson, 1984). Although these two types of networks have phenomenologic similarities, a consideration of the problem of cell movement in terms of a network composed of stiff rods may generate new physical insights.

APPENDIX

Thermodynamics of Actin Filament Solutions Subjected to Osmotic Stress

The osmotic stress on the solution in the osmometer is due to an imbalance of osmolarity between the inside and the outside. This Appendix shows that the osmotic stress not only produces volume flow in a polymer solution but also couples thermodynamically with a mechanical force to deform the polymer. Furthermore, a quantitative relationship between the osmotic stress and the compression is shown without any special assumption about mechanical and dynamic properties of the polymer.

Profile of the Chemical Potential of Water. An evaluation of the chemical potential of water is essential for the thermodynamic analysis. Fig. 9 diagrams the chemical potential profile of water predicted at steady state after changing the osmolarity in compartment II by adding dextran. Stirring of the solution in compartment II rapidly dissipates the dextran concentration gradient so that there is no chemical potential gradient of water in compartment II. If the membrane is homogeneous, i.e., if the frictional coefficient on a water molecule in the membrane is constant at any point, the chemical potential gradient of water should be constant through the membrane (Katchalsky and Curran, 1965). The membrane used is expected to be homogeneous. The chemical potential profile of water in compartment I can be evaluated as follows. The volume flow of water at steady state is equal to $(\phi_w/f_w)\,(du_w/dx)$, where f_w, ϕ_w, and du_w/dx represent the frictional coefficient on a water molecule, the volume fraction of water, and the chemical potential gradient of water, respectively. Since the flow must be continuous at the boundary between the membrane and compartment I, it follows that

$$\frac{\phi_w^I}{f_w^I}\left(\frac{du_w(0)}{dx}\right)^I = \frac{\phi_w^m}{f_w^m}\left(\frac{du_w(0)}{dx}\right)^m,$$

i.e.,

$$\left(\frac{du_w(0)}{dx}\right)^I = \frac{\phi_w^m/f_w^m}{\phi_w^I/f_w^I}\left(\frac{du_w(0)}{dx}\right)^m, \qquad (1A)$$

where $(du_w(0)/dx)$ represents the gradient at the boundary and the superscripts of m and I denote the values in the membrane and in compartment I. The gradient in compartment I should have a maximum value at the boundary because the gradient is made by changing the

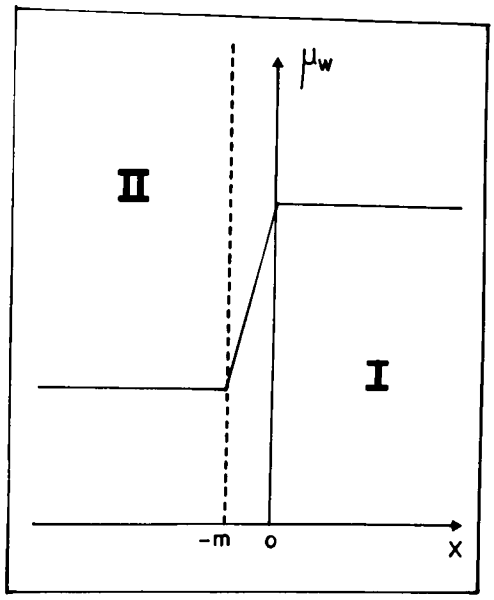

FIGURE 9 The profile of chemical potential of water in the system at steady state. The chemical potential is plotted as a function of position. Compartment I, which is inside of the osmometer, is $x > 0$. The membrane itself is $-m \le x \le 0$. Compartment II, which is the external buffer bath, is $x < -m$.

osmolarity in compartment II. Therefore,

$$\left(\frac{du_w(x)}{dx}\right)^{I} \leq \frac{\phi_w^m/f_w^m}{\phi_w^I/f_w^I}\left(\frac{du_w(0)}{dx}\right)^{m}, \qquad (2A)$$

where $(du_w(x)/dx)^I$ is the gradient to an arbitrary point of compartment I. To evaluate the value of $(du_w(x)/dx)^I$ from Eq. 2A, we need the values of ϕ_w^m/f_w^m and ϕ_w^I/f_w^I. The value of f_w^m/ϕ_w^m, for the membrane used, is 3.3×10^{13} dyn s/cm mol from the experimental value of the filtration coefficient taking 90 μm as the membrane thickness. The value of f_w^I is calculated as follows. It can be shown from Onsager's law that the ratio of the frictional coefficient on a solute molecule, f_s, to that on a solvent molecule, f_w, is equal to the inverse of the molar ratio of the solute molecules to the solvent molecules, m, i.e., $f_w = mf_s$. From Stoke's law, $f_s = 6.02 \times 10^{23} \times 6\pi r\eta$, where r and η represent the radius of the solute molecule and the viscosity of the solvent, respectively. In a solution of 10 mg/ml G-actin, taking 20 nm as the value of r, f_w can be calculated to be 1×10^{11} dyn s/cm mol. The value of f_w for an F-actin solution must be smaller since the contact area of a G-actin molecule with water is larger than that of a subunit molecule in an F-actin filament. The value of ϕ_w^I can be assumed to be unity in the solution. Therefore, the following relation can be maintained in an actin solution of 10 mg/ml

$$\left(\frac{du_w(x)}{dx}\right)^{I} \leq 3.0 \times 10^{-3}\left(\frac{du_w(0)}{dx}\right)^{m}. \qquad (3A)$$

Eq. 3A indicates that the gradient in a 10 mg/ml actin solution is <0.3% of the gradient in the membrane so that it can be considered negligible. From the analysis described above, the chemical potential of water at steady state in our system is like the one shown in Fig. 9, in which the gradient produced by the osmolarity change exists only in the membrane and not in either compartment I or compartment II. This conclusion allows us to treat the solution in compartment I as a thermodynamically homogeneous system at steady state, i.e., as a partial equilibrium system that can be described by thermodynamic functions at equilibrium.

Analysis of the Forces Acting on a Filamentous Polymer. The compression of the actin filaments by osmotic stress is a thermodynamic phenomenon in which osmotic work is transformed into mechanical work that compresses the filaments. It can be analyzed as follows. We shall consider a filament stretched to an extent, dl, by a force, f, and shall assume that the osmotic work occurs in compartment I simultaneous to the flow of water under the influence of the chemical potential difference of water between the two compartments, Δu_w. The free energy change of the solution in compartment I accompanying the simultaneous stretch and water movement is

$$dG = n_f f\,dl - \Delta u_w\,dn_w, \qquad (4A)$$

where n_f and n_w are the number of filaments and moles of water, respectively. Δu_w can be represented as $\bar{V}_w \Delta P_o$, where $\bar{V}_w$ is the molar volume of water, and ΔP_o is the chemical potential difference of water in pressure units. Therefore

$$\begin{aligned} dG &= n_f f\,dl - \Delta P_o\,dV_w \\ &\simeq n_f f\,dl - \Delta P_o\,dV, \end{aligned} \qquad (5A)$$

where V_w and V are the volume of water and volume of solution, respectively, in compartment I, and it is assumed that $n_w\bar{V}_w = V_w \simeq V$. Initially, the whole system is in equilibrium. However, after the osmolarity of the solution in compartment II is changed, a volume flow of water occurs from compartment I to compartment II, which continues until the system arrives at a new equilibrium at infinite time. We define an osmotic stress, P_f, as

$$P_f = \Delta P_h - RT\Delta C,$$

where ΔP_h and ΔC represent the hydrostatic pressure difference and the concentration difference of the dextran between compartment I and compartment II. The value of P_f at equilibrium is zero since ΔP_h becomes equal to $RT\Delta C$. The differential of P_f at steady state, where s and d_w represent the cross-sectional area of the osmometer capillary and the density of the solution, respectively, is

$$dP_f = d\Delta P_h = (d_w/s)\,dV \qquad (6A)$$

since the change of ΔC accompanying the volume flow is negligible. Using Eq. 6A, Eq. 5A can be rewritten as

$$dG = n_f f\,dl - (s/d_w)\,\Delta P_o\,dP_f. \qquad (7A)$$

We represent the free energy of the solution in compartment I at steady state as $G(\Delta l, P_f)$ and at equilibrium at infinite time as $G(0, 0)$. The free energy at steady state near equilibrium is treated according to the procedure of Meixner (1949). Expansion of the free energy in a Maclaurin series, retaining only quadratic terms, yields the following equations:

$$\begin{aligned} G(\Delta l, P_f) = G(0,0) &+ \frac{1}{2}\left(\frac{\partial^2 G}{\partial l^2}\right)^{\circ}_{P_f}(\Delta l)^2 \\ &+ \frac{1}{2}\left(\frac{\partial^2 G}{\partial l \partial P_f}\right)^{\circ}\Delta l P_f + \frac{1}{2}\left(\frac{\partial^2 G}{\partial P_f^2}\right)^{\circ}_{l}(P_f)^2 \end{aligned} \qquad (8A)$$

since $(\partial G/\partial l)^{\circ}_{P_f} = 0$ and $(\partial G/\partial l)^{\circ}_{l} = 0$ at equilibrium. The superscript 0 on the differentials indicates that these are equilibrium values. We can obtain the following equations from Eqs. 7A and 8A:

$$\begin{aligned} \left(\frac{\partial G}{\partial l}\right)_{P_f} = n_f f &= \left(\frac{\partial^2 G}{\partial l^2}\right)^{\circ}\Delta l + \left(\frac{\partial^2 G}{\partial l \partial P_f}\right)^{\circ} P_f \\ &= n_f\left(\frac{\partial f}{\partial l}\right)_{P_f}\Delta l + n_f\left(\frac{\partial f}{\partial P_f}\right)_{l} P_f \end{aligned} \qquad (9A)$$

$$\begin{aligned} \left(\frac{\partial G}{\partial P_f}\right)_{l} = -\frac{s}{d_w}\Delta P_o &= \left(\frac{\partial^2 G}{\partial l \partial P_f}\right)^{\circ}_{P_f}\Delta l + \left(\frac{\partial^2 G}{\partial P_f^2}\right)^{\circ} P_f \\ &= -\frac{s}{d_w}\left(\frac{\partial \Delta P_o}{\partial l}\right)\Delta l - \frac{s}{d_w}\left(\frac{\partial \Delta P_o}{\partial P_f}\right)_{l} P_f \end{aligned} \qquad (10A)$$

$$n_f\left(\frac{\partial f}{\partial P_f}\right)_{l} = \left(\frac{\partial^2 G}{\partial l \partial P_f}\right)^{\circ} = \frac{s}{d_w}\left(\frac{\partial \Delta P_o}{\partial l}\right)_{P_f}. \qquad (11A)$$

In Eq. 10A, $(\partial \Delta P_o/\partial P_f) = 1$ since the change of ΔP_o at steady state under constant l is simply equal to the change of hydrostatic pressure, which is equal to the change of P_f as shown in Eq. 6A. $(\partial \Delta P_o/\partial l)_{P_f}\Delta l$ corresponds to the elastic pressure ΔP_e, since

$$\begin{aligned} \Delta P_e &= \int_0^{\Delta l}\left(\frac{\partial \Delta P_o(\Delta l)}{\partial l}\right)_{P_f} d(\Delta l) \\ &\simeq \left(\frac{\partial \Delta P_o(0)}{\partial l}\right)_{P_f}\Delta l. \end{aligned} \qquad (12A)$$

The approximation in Eq. 12A is of the same order as those in Eqs. 9A and 10A. The discussions above lead to the following equation from Eq. 10A:

$$\Delta P_o = \Delta P_e + P_f. \qquad (13A)$$

In Eq. 9A, the first term is related to the hydrostatic pressure as follows:

$$\left(\frac{\partial f}{\partial l}\right)_{P_f} \Delta l = S_f E \frac{\Delta l}{l_o} = S_f(P_h - P_h^{eq}), \quad (14A)$$

where E, l_o, S_f, P_h, and P_h^{eq} represent Young's modulus, the length, the cross-sectional area of the filament, and the hydrostatic pressures at steady state and at equilibrium, respectively. The second term can be related to the elastic pressure with the cross relation shown in Eq. 11A

$$n_f\left(\frac{\partial l}{\Delta P_f}\right)_l = -\frac{s}{d_w}\left(\frac{\partial \Delta P_o}{\partial l}\right)_{P_f} \Delta l = -\frac{s}{d_w}\Delta P_e$$

$$n_f\left(\frac{\partial f}{\Delta P_f}\right)_l P_f = -\frac{S}{d_w}\frac{P_f}{\Delta l}\Delta P_e. \quad (15A)$$

Inserting Eqs. 14A and 15A into Eq. 9A, we obtain

$$f = S_f(P_h - P_h^{eq}) - \frac{1}{n_f}\frac{s}{d_w}\frac{P_f}{\Delta l}\Delta P_e.$$

In the experiments expected here, $(P_h - P_h^{eq})$ is <30 cm H_2O and can, therefore, be neglected. Therefore,

$$f = -\frac{1}{n_f}\frac{s}{d_w}\frac{P_f}{\Delta l}\Delta P_e \quad (16A)$$

or

$$\Delta P_e = -\frac{n_f d_w}{s} f \frac{\Delta l}{P_f}. \quad (17A)$$

ΔP_e is derived in another way from the free energy of deformation of the filament ΔF_d as follows (Flory, 1953)

$$\Delta P_e = -\left(\frac{\partial \Delta F_d}{\partial V}\right)_{n_f} = -\left(\frac{\partial \Delta F_d}{\partial \Delta l}\frac{\partial \Delta l}{\partial V}\right)_{n_f} = -\frac{n_f d_w}{s} f\left(\frac{\partial \Delta l}{\partial P_f}\right)_{n_f} \quad (18A)$$

since Eqs. 17A and 18A should be equal to each other,

$$\left(\frac{\partial \Delta l}{\partial P_f}\right) = \frac{\Delta l}{\Delta P_f}, \quad (19A)$$

i.e., $\Delta l/P_f$ is constant at a constant concentration of filaments. According to Hook's law, f is proportional to l, and so is proportional to P_f, that is,

$$f = \text{constant} \times P_f. \quad (20A)$$

Considering the relations shown in Eqs. 19A and 20A on Eq. 17A, we get,

$$\Delta P_e = -\epsilon P_f, \quad (21A)$$

where ϵ is constant at a constant filament concentration. From Eqs. 13A, 16A, and 21A,

$$f = \frac{\epsilon s}{n_f d_w}\frac{P_f}{\Delta l}P_f = \frac{\epsilon s}{n_f d_w}\left(\frac{\partial \Delta P_f}{\partial l}\right)P_f \propto P_f \quad (22A)$$

$$\Delta P_o = \Delta P_e + P_f = (1 - \epsilon)P_f. \quad (23A)$$

Eq. 22A shows that a change in P_f, which can be manipulated experimentally, affects linearly the force acting on the filaments. As shown in Eq. 21A, ϵ is a parameter of the elastic response of the filament to the osmotic stress and is related to the elastic properties of the filament as follows. From Eq. 22A,

$$\frac{f/s_f}{(\Delta l/l_o)} = \frac{\epsilon s}{s_f n_f l_o d_w}\left(\frac{P_f}{\Delta l/l_o}\right)^2 = \frac{\epsilon s}{s_f n_f l_o d_w}\frac{1}{E_o^2} = E, \quad (24A)$$

where E is Young's modulus and E_o represents $P_f//\Delta l/l_o$, which can be called the modulus of the osmotic compression by analogy to Young's modulus. It is constant at constant concentration of the filaments as discussed previously. From Eq. 24A,

$$\epsilon = \frac{n_f V_f}{s} d_w \frac{E}{E_o^2} = \frac{V}{s}\Phi d_w \frac{E}{E_o^2}, \quad (25A)$$

where Φ is the volume fraction of the filament. Eq. 25A shows that ϵ is proportional to Young's modulus and the square inverse of the modulus of the osmotic compression. The free energy of the deformation F_d can be calculated from Eq. 22A

$$\Delta P_f = \int_0^{\Delta l/l_o} = \frac{\epsilon s}{n_f d_w}\int_0^{\Delta l}\frac{dP_f}{dl}P_f dl = \frac{\epsilon s}{n_f d_w}\int_0^{P_f} P_f dP_f = \frac{\epsilon s}{2 n_f d_w}P_f^2, \quad (26A)$$

that is, the free energy is proportional to ϵ and square of the intensity of the osmotic force, P_f. The value of ϵ can be evaluated experimentally as follows. Under the condition that the chemical potential of water has a characteristic profile as shown in Fig. 9, the volume flow of water through the membrane, J_v, which is equivalent to the volume flow of a solution in compartment I, is related directly to ΔP_o

$$J_v = L_p \Delta P_o, \quad (27A)$$

where L_p is a characteristic value of the membrane. From Eqs. 21A and 27A,

$$J_v = L_p(1 - \epsilon)P_f,$$

or

$$\frac{(J_v/P_f)}{(J_v^o/P_f)} = (1 - \epsilon),$$

where J_v^o is the volume flow of an ideal solution that shows no elastic response to the osmotic stress. Therefore, ϵ can be obtained by comparing the value of each slope of $J_v - P_f$ curve between the test polymer solution and the ideal solution.

The authors wish to express their gratitude to Dr. George Oster for many useful discussions and suggestions about these studies. We also acknowledge the useful comments of Drs. T. Tanaka and P. Janmey.

This work supported by National Heart, Lung and Blood Institute grants HL-19429 and HL-00912 and grants from the Council for Tobacco Research and the Edwin S. Webster Foundation. Dr. Ito was the recipient of grants from the Kyoto University 70th Anniversary Memorial Foundation and the Yamada Science Foundation.

Received for publication 21 April 1986 and in final form 7 November 1986.

REFERENCES

Chapponier, C., P. Janmey, and H. Yin. 1986. The actin filament severing domain of gelsolin. *J. Cell Biol.* 103:1473–1481.

Edwards, S., and K. Evans. 1982. Dynamics of highly entangled rod-like molecules. *J. Chem. Soc. Faraday Trans II.* 78:113–121.

Flory, P. 1953. Principles of Polymer Chemistry. Cornell University Press, Ithaca. 541–594.

Flory, P. 1956*a*. Statistical thermodynamics of semi-flexible chain molecules. *Proc. Roy. Soc. Edinb. Sect. A.* (*Math. Phys. Sci.*). 234:60–73.

Flory P. 1956*b*. Phase equilibria in solutions of rod-like particles. *Proc. Roy. Soc. Edinb. Sect. A.* (*Math. Phys. Sci.*). 234:73–89.

Katchalsky, A., and P. Curran. 1965. Nonequilibrium Thermodynamics in Biophysics. Harvard University Press, Cambridge.

Meixner, J. 1943. Zur Thermodynamick der irreversiblen Prozesse in Gasen mit chemisch reagierden, dissoziierenden und anregbaren Komponenten. *Ann. Phys.* 43:244–270.

Oster, G. 1984. On the crawling of cells. *J. Embryol. Exp. Morphol.* 83 (Suppl.):329–364.

Oster G., and A. Perelson. 1985. Cell spreading and motility: a model lamellipod. *J. Math. Biol.* 21:383–388.

Schmid-Schonbein, G. W., K. P. Sung, H. Tozeren, R. Skalak, and S. Chien. 1981. Passive mechanical properties of human leukocytes. *Biophys. J.* 36:243–256.

Spudich, J., and S. Watt. 1971. The regulation of rabbit skeletal muscle contraction. *J. Biol. Chem.* 246:4866–4871.

Stossel, T. 1984. Contribution of actin to the structure of the cytoplasmic matrix. *J. Cell Biol.* 99:15s–21s.

Tait, J., and C. Frieden. 1982. Polymerization and gelation of actin studied by fluorescence photobleaching recovery. *Biochemistry.* 21:3666–3674.

Tanaka, T. 1981. Gels. *Sci. Am.* 244:124–138.

Tanaka, T., and D. Fillmore. 1979. Kinetics of swelling of gels. *J. Chem. Phys.* 70:1214–1218.

Zaner, K. S., and T. P. Stossel. 1982. Some perspectives on the viscosity of actin filaments. *J. Cell Biol.* 93:987–991.

Zaner, K., and T. Stossel. 1983. Physical basis of the rheologic properties of F-Actin. *J. Biol. Chem.* 258:11004–11009.

Zaner, K. 1986. The effect of the 540 kilodalton actin crosslinking protein, actin binding protein (ABP) on the mechanical properties of F-actin. *J. Biol. Chem.* 261:7615–7620.

Zimm, B., and I. Myerson. 1946. A convient small osmometer. *J. Am. Chem. Soc.* 68:911–912.